A Machine Learning-Based Portable Inspection Method for Evaluation of Tool Surface Condition and Release Coating in Composites Manufacturing

Caleb Schoenholz; Shuangshan Li; Kyle Bainbridge; Vy Huynh; Alex Gray; Xu Chen; Navid Zobeiry

DOI: https://doi.org/10.33599/nasampe/s.22.0740

SAMPE publication page

RELATED JOURNAL PUBLICATION

Related expanded open-access journal article: Accelerated In Situ Inspection of Release Coating and Tool Surface Condition in Composites Manufacturing Using Global Mapping, Sparse Sensing, and Machine Learning, Journal of Manufacturing and Materials Processing 7(3) (2023), 81, https://doi.org/10.3390/jmmp7030081

A MACHINE LEARNING-BASED PORTABLE INSPECTION METHOD FOR EVALUATION OF TOOL SURFACE CONDITION AND RELEASE COATING IN COMPOSITES MANUFACTURING

Caleb Schoenholz[1], Shuangshan Li[1], Kyle Bainbridge[1], Vy Huynh[1], Alex Gray[1], Xu Chen[2], Navid Zobeiry[1]

[1]Materials Science & Engineering Department, University of Washington

302 Roberts Hall, Box 352120

Seattle, WA 98195-2120, U.S.A.

[2]Mechanical Engineering Department, University of Washington
3900 E Stevens Way NE, Box 352600

Seattle, WA 98195-2120, U.S.A.

ABSTRACT

During composites manufacturing, release coatings are applied on production tools to minimize tool-part friction and adhesive bonding. In addition to facilitating the removal of cured parts, applying release coatings reduces process-induced deformations (PIDs). The aerospace industry typically uses semi-permanent release coatings that undergo physical and chemical changes (i.e., aging) with each processing cycle. Fresh layers are frequently reapplied on top of aged coats to mitigate aging effects. Due to a lack of knowledge on the relationship between processing and aging, reapplications of release coating are often untimely and consequently lead to cost-deficient tool preparation schedules, or excessive PIDs. This paper presents a novel machine-learning (ML) framework to evaluate the condition of release coating using non-destructive and portable Fourier-transform infrared spectroscopy (FTIR) and contact angle goniometry (CAG). ML methods and other numerical tools are used to connect measurements gained from low-precision portable equipment to results obtained from high-precision laboratory instruments. The accuracy and portability of the technique demonstrates potential for scale-up and implementation into an automated industrial process. The research results contributes to understand the aging mechanisms of release coating, improve the efficiency of tool cleaning and preparation, and potentially mitigate PIDs in composites manufacturing.

Keywords: Composites Manufacturing, Tooling Inspection, Machine Learning
Corresponding author: Navid Zobeiry

1. INTRODUCTION

Aerospace composites manufacturing consists of complex and interdependent processes that may contribute to the formation of residual stresses and consequently process-induced deformations (PIDs) [1,2]. Residual stresses are formed during processing mainly due to a mismatch of free strains at the micro-, macro-, coupon-, and component-levels [3]. Other factors, however, may also contribute to the formation of residual stresses and PIDs including tool-part interaction [3-13] in the form of interfacial bonding and/or friction. To mitigate minimize residual stress formation and PIDs induced by tool-part interaction, tools are typically prepared with release coatings prior to part lay-up. Release coatings also facilitate the removal of cured parts after processing [14].

Preparing a tool with release coating in composites manufacturing typically consists of three sequential steps. First, the production tool is treated with solvent-based mold cleaner to remove any residue from previous processing or handling (Fig. 1a). Depending on the severity and amount of resin residue, abrasive cleaning methods (e.g., coarse pads), or nonabrasive industrial methods such as dry ice blasting may be used in addition to solvent cleaning. This, however, may increase the tool surface roughness and consequently tool-part interaction. Next, a mold sealer is applied directly on the tool surface to create a smooth base layer by covering micro-cavities and scratches , and prevent mechanical interlocking (i.e., physical bonding) between the tool and part (Fig. 1b). Then, several layers of release agent (RA) are applied on top of the sealed surface to form a low-energy barrier that prevents the formation of strong adhesive bonds and minimizes tool-part friction (Fig. 1c) [14]. Mold sealer and release agent combine to form an abhesive and impenetrable release coating between the tool and part during lay-up (Fig. 1d) and processing.

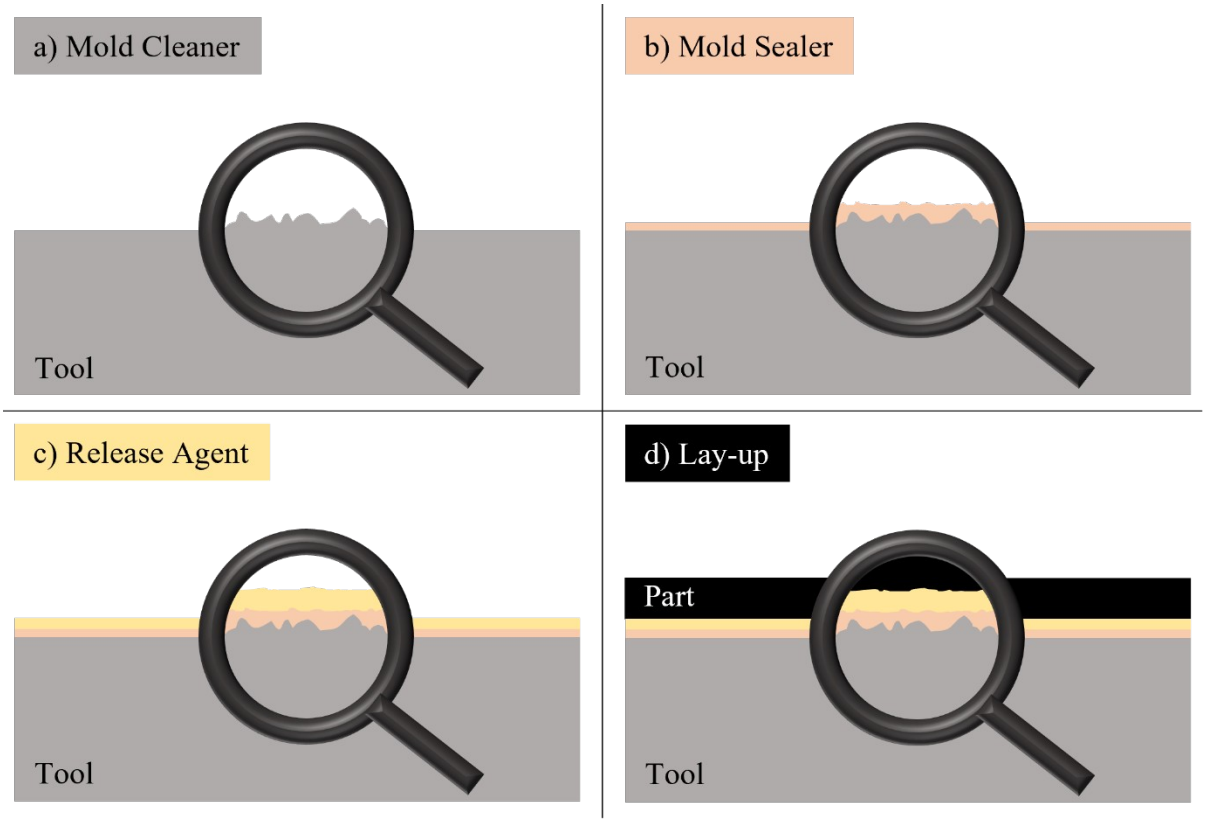

Figure 1. Sequential steps of tool preparation and prepreg lay-up in composites manufacturing. a) Remove residue with mold cleaner. b) Fill-in surface pores and scratches with mold sealer. c) Minimize surface free energy with release agent. d) Lay-up prepreg plies on coated tool surface.

The aerospace industry typically uses silicone-based release coatings due to their low adhesion (i.e., high abhesion) and high thermal/chemical stability properties. Silicone-based coatings are usually applied as liquids and cured through an evaporation reaction to form thin polymer barriers. During the cross-linking reaction of thermoset composites, some release coating small molecules and monomers transfer from tool to part surface and are physically and chemically integrated into the part's resin network. The transfer of molecules decreases the thickness of the remaining coating layer on the tool surface [15]. Elevated temperatures and pressures during autoclave processing may also cause resin to bleed from the prepreg or get stuck in cavities of tool surface during demolding process and hence contaminate the tool. Consequently, each successive processing cycle results in a further reduction of coating thickness, an increase of its contamination level, and thus, a decrease in overall abhesion properties. The resultant change in physical/chemical properties due to processing can be considered as the "aging" of release coating. The aging of release coating may strongly influence the level of tool-part interaction, residual stresses, and PIDs.

A common method utilized to mitigate aging and maintain effective abhesion properties is to frequently reapply fresh layers of release agent on top of the aged coating in between processing cycles. Mold sealers are seldom reapplied on top of aged coats due to their inherently long cure times, but release agents (RAs) typically can be reapplied in relatively short periods of time. The frequency of RA reapplications and tool surface cleaning in the production environment is often based on tacit and know-how knowledge . This often leads to a high frequency of RA reapplications in process specifications to ensure successful demolding of parts. In addition to cost considerations and reducing production rate, reapplying too many RA layers may affect the quality of parts [15,16]. Conversely, too few reapplications could lead to costly problems such as excessive PIDs or parts that are not demoldable after processing. Another approach that may be used to mitigate aging effects is to completely clean the tool using methods such as dry-ice blasting and retreat it with fresh layers of mold sealer and RA. However, this latter method is particularly disruptive to the flow of manufacturing and is therefore only used when tools are highly contaminated and need thorough cleaning.

Evaluating tool surface condition and release coating in real-time using non-destructive portable analysis equipment may reduce untimely RA reapplications and improve the efficiency of tool preparation. Two widely-utilized tools in the aerospace industry for non-destructive surface characterization of composites are Fourier-transform infrared spectroscopy (FTIR) and contact angle goniometry (CAG) [17,18]. The recent advent of handheld FTIR and CAG instruments makes the techniques even more viable as quick analysis methods to implement into manufacturing processes. However, measurements gained from portable equipment often lack in precision compared to results obtained from scientific-grade laboratory instruments due to differences in sampling methods and overall equipment capabilities [18]. The lack of precision in portable equipment may result in false-positive or false-negative tool surface evaluation during manufacturing. A robust tool evaluation approach may be developed by taking advantage of machine-learning (ML) techniques to connect measurements gained from low-precision portable equipment to results obtained from high-precision laboratory instruments. This paper presents a

novel ML framework to evaluate tool surface condition and release coating using non-destructive and portable FTIR and CAG. Tool surface chemistry and free energy are characterized as functions of process variables including the number of RA layers, processing cycles, and RA reapplications. Contamination levels on tool surfaces are also visually monitored throughout testing. The combined portable experimental techniques and ML analysis technology can be implemented at an industrial setting for fast and automated evaluation of large production tools.

2. EXPERIMENTATION

2.1 Materials

The release coating used in this study consisted of two components: Loctite® Frekote® B-15™ mold sealer and 710-NC™ release agent. The exact formulations of Frekote products are proprietary, but basic information is listed on publicly available data sheets [20,21]. The composition by weight of Frekote B-15 mold sealer includes 1-5% silicone components (reaction product of TMAS and PDMS) and 90-100% dibutyl ether as the solvent. The composition by weight of Frekote 710-NC release agent includes 1-5% silicone components (reaction product of TMAS and PDMS), 1-5% octane, 1-5% hydrocarbons (C7-10), 60-100% petroleum as the carrier, and 10-30% dibutyl ether as the solvent. After the release coating components are applied on tool surfaces, most of the carrier and solvent evaporate, while the silicones and hydrocarbons remain on the tool surface. Polydimethylsiloxane (PDMS) acts as the active silicone in Frekote mold sealer and release agent [14]. PDMS allows for chemical compatibility between the two release coating products, high abhesion (i.e., low surface free energy), and high chemical/thermal stability.

For composites manufacturing, Toray T800S/3900-2 UD prepreg was used. 3900-2 is a toughened aerospace-grade epoxy resin, while T800S is an intermediate modulus and high strength carbon fiber. In addition to epoxy resin, surface of the prepreg is partially covered with micro-spherical thermoplastic tougheners. Composite parts were fabricated on prepared tools to age the release coating and evaluate the tool surface condition after each manufacturing cycle. For processing, a temperature cycle consists of heating to 180°C at 2°C/min and hold at 180°C for 120 minutes before cool-down was used. A pressure of 0.7 MPa was applied throughout processing.

2.2 Method

The test method consisted of fifteen sequential rounds of autoclave processing followed by FTIR and CAG surface analysis. Portable analysis methods were used on two large-scale production tools, while laboratory instruments were utilized on small-scale test coupons with similar surface conditions as production tools. One-half of the coupons were analyzed using FTIR, and the others were used for CAG testing. Each production tool was divided into three sections containing varying amounts of RA. Coupons were prepared to mimic each surface condition and underwent autoclave processing cycles alongside production tools. The portability of the coupons allowed for high-precision laboratory analysis of each surface condition. FTIR and CAG testing were conducted after each cycle for the first five cycles, then after every five cycles through the remainder of the campaign. The two production tools were prepared to have identical surface conditions prior to any autoclave processing. Throughout testing, one tool and set of coupons were treated with one fresh layer of RA after every three cycles, while no RA reapplications were conducted on the other tool.

2.3 Sample Preparation

Two Invar plates with approximate dimensions of 3 mm (t) × 300 mm (w) × 600 mm (l) were used as production tools. Twelve Invar coupons were made by cutting 25 mm (w) × 25 mm (l) square sections from a 0.25 mm-thick Invar sheet. Approximately three-fourths of each production tool was used as a lay-up surface, while the other one-fourth was used to support six coupons during processing. Samples were prepared using the following procedure:

Step 1: Both production tools and all coupons were cleaned with Loctite® Frekote® PMC™ mold cleaner to remove any surface residue from previous cutting or handling.

Step 1: Two layers of mold sealer were applied to the lay-up surfaces of each production tool and coupon using a lint-free cotton wiping cloth, allowing 30 minutes between coats. Then, the production tools and coupons were placed in a convection oven for 60 minutes at 95 °C.

Step 3: For each tool, the lay-up area was divided into three sections. The sections were prepared with either one, three, or five layers of RA. A lint-free cotton wiping cloth was used to apply RA layers, allowing 15 minutes between coats. The set of twelve test coupons were similarly prepared with either one, three, or five layers of RA using the same technique. Four coupons were treated with one layer, four were treated with three layers, and the other four were treated with five layers of RA. Two coupons with each surface condition (i.e., one, three, five layers of RA) were adhered to the unsealed sections of each production tool using flashbreaker tape.

Step 4: One ply of Toray T800S/3900-2 UD prepreg with nominal dimensions of 250 mm (w) × 400 mm (l) was laid-up to cover the release-coated areas on each production tool surface. Then, one 20 mm (w) × 20 mm (l) ply of UD prepreg was laid-up on each coupon.

Step 5: Each production tool and set of coupons was covered with one sheet of fluorinated ethylene propylene (FEP) release film, followed by one layer of breather. The tools and lay-ups were placed and sealed in separate vacuum envelope bags (produced by Torr Technologies, Inc.), loaded into an autoclave, and subjected to the Manufacturer's Recommended Cure Cycle (MRCC).

Step 6: Once the cure cycle was complete, the envelope bags were removed from the autoclave and all composite parts were demolded from the tools and coupons. Test coupons were removed from the production tools and stored in sealed bags until taken for laboratory analysis.

Step 7: Steps 4-6 were repeated before each round of testing for a total of fifteen rounds. One of the production tools and set of six coupons were treated with one fresh layer of RA every three cycles. The other tool and coupons underwent all fifteen rounds of autoclave processing without any RA reapplications.

2.4 Tool Surface Chemistry Measurements

2.4.1 Fourier-Transform Infrared Spectroscopy (FTIR)

Surface chemistry measurements were conducted after autoclave processing cycles using portable and laboratory FTIR spectrometers on production tools and coupons, respectively. Portable FTIR

measurements were performed using an Agilent Technologies 4100 ExoScan handheld FTIR on the basis of diffuse reflectance. The handheld FTIR was mounted onto optomechanical components that allowed for three-dimensional portability over a production tool surface (Fig. 2). Laboratory FTIR measurements were conducted on test coupons using a Bruker Vertex 70 FTIR Spectrometer on the basis of attenuated total reflectance (ATR). Three IR-absorbance spectra were scanned in different areas of each production tool surface condition and coupon in the range of 500-4000 cm^{-1}. The three spectra were normalized, averaged, and plotted for analysis.

2.5 Tool Surface Free Energy Measurements

2.5.1 Contact Angle Goniometry (CAG)

Surface free energy (SFE) measurements were conducted using a novel portable CAG method on production tools in conjunction with a well-established laboratory method on coupons. The portable CAG method utilized a manual liquid drop dispensing technique that was only sufficient for polar liquids with relatively low sensitivity to drop size. Laboratory analysis was used for the dispersive components that require highly controlled liquid drop dispensing [22]. Di-ionized water (DI water) and diiodomethane (DIM) were used as the polar and dispersive liquids, respectively.

The portable CAG set-up consisted of mounting a miniature digital microscope onto optomechanical components alongside the portable FTIR (Fig. 2). Five droplets of DI water with approximate volumes of 50 µL were manually dispensed using a pipette on each production tool surface condition. A VCA Optima video contact angle system was utilized for laboratory analysis of DIM droplets. Five droplets of DIM with volumes of 1 µL were dispensed on the test coupons using an automated syringe system. Side-view images of each droplet were captured immediately after solid-liquid contact on the production tools and coupons. Contact angles were calculated from portable analysis images using ImageJ processing software. Laboratory-generated contact angles were calculated from the VCA system's software. Five contact angles for each liquid were used to calculate SFE using the Owens-Wendt method [23]. The dispersive and polar tensions of DI water were assumed to be 22.1 dyne/cm and 50.7 dyne/cm, respectively. The dispersive and polar tensions of DIM were assumed to be 48.5 dyne/cm and 2.3 dyne/cm, respectively.

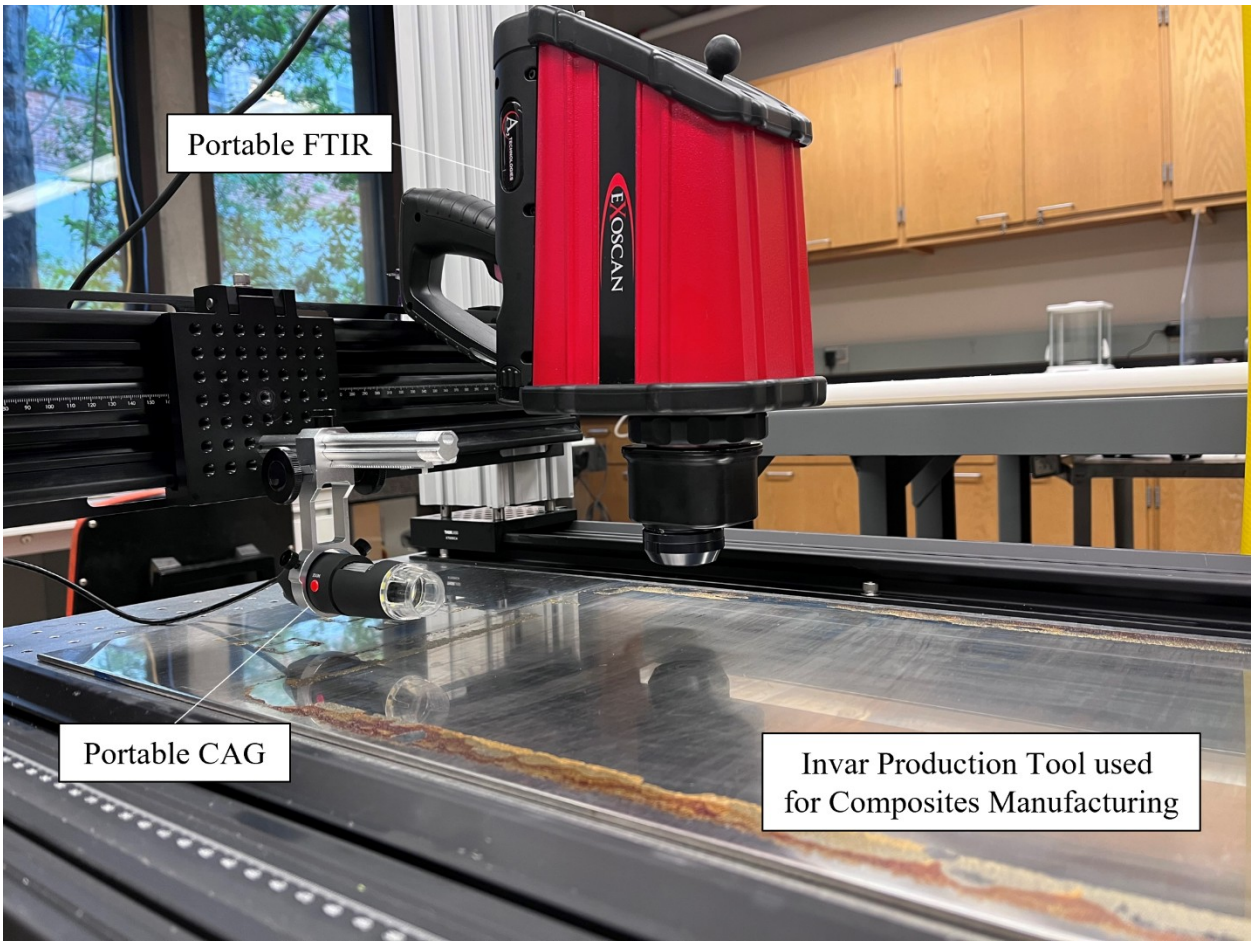

Figure 2. Portable tool surface analysis set-up used to measure surface free energy and surface chemistry; digital microscope used for contact angle goniometry (CAG) (left) and an Agilent Technologies 4100 ExoScan handheld FTIR (right).

3. RESULTS

3.1 Tool Surface Chemistry

Figure 3 shows IR-absorbance spectra of a tool surface covered in two layers of mold sealer and three layers of RA prior to any composites processing and after five cycles. The bottom spectrum was measured on a production tool using the portable FTIR, while the top spectrum was measured on a test coupon using the laboratory FTIR. Both plots exhibit the same general peaks at wavenumbers of 2960, 2920, 2850, 1470, 1260, 1090, 1020, and 780 cm^{-1}. The four peaks at wavenumbers 780, 1020, 1090, and 1260 cm^{-1} are characteristic of silicone materials – specifically a PDMS polymer network [14,15,18,19]. The peak at 780 cm^{-1} represents Si-CH_3 bond stretching. The peaks at 1020 and 1090 cm^{-1} represent the asymmetric stretching of Si-O-Si bonds. The peak at 1260 cm^{-1} is characteristic of the symmetrical deformation of the C-H bond in the Si-$(CH3)_2$ groups (i.e., Si-CH_3 bending). Both spectra also exhibit a peak at 1470 cm^{-1} and a cluster of peaks around 2920 cm^{-1} which represent C-H scissoring and asymmetric C-H stretching, respectively. Although the portable and laboratory techniques identified characteristic IR-peaks at

similar wavenumbers, there were significant differences in absorbance spectra. First, the scale of portable IR-absorbance was approximately two-fold larger than laboratory results. Additionally, the pattern of change in peak intensity with processing cycles was opposite between portable and laboratory results. FTIR peaks were decreased with release coating aging in portable analysis and increased with laboratory measurements. The differences in peak intensities and behavior with aging is likely due to differences in sampling methods between portable and laboratory equipment.

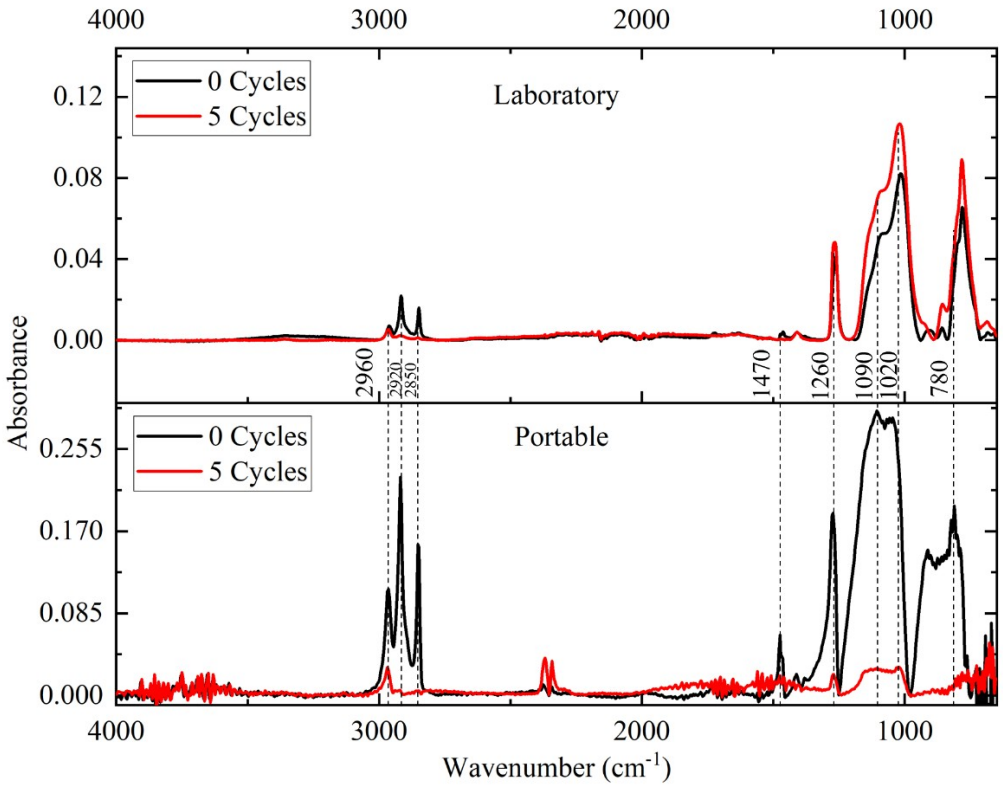

Figure 3. IR-absorbance spectrum of tool surface with two layers of Frekote mold sealer and three layers of release agent using portable and laboratory FTIRs.

Connecting portable to laboratory FTIR results consisted of calculating a fitting-ratio for each of the absorbance peaks. The fitting-ratio was calculated by dividing the laboratory peak intensity by its portable counterpart. Fig. 5 shows a fitting-ratio for the 780 cm^{-1} absorbance peak versus the number of RA layers and processing cycles. Red points in the plot represent calculated fitting-ratios from experimental IR-peak measurements. A response surface, shown in green, was fitted to the data using Gaussian Process Regression (GPR) method with an accuracy of 86%. The response surface shows the ratio between portable and laboratory absorbance intensities for the 780 cm^{-1} peak changes with processing cycles and RA layers. There is a direct increase in fitting-ratio with processing cycles, followed by a plateau for all number of layers of RA. If the tool surface history including the number of RA layers and processing cycles are known, the fitting-ratio can be used as a direct link to transform portable FTIR measurements into laboratory values. The laboratory values can then be used to measure the age of release coating on a tool surface.

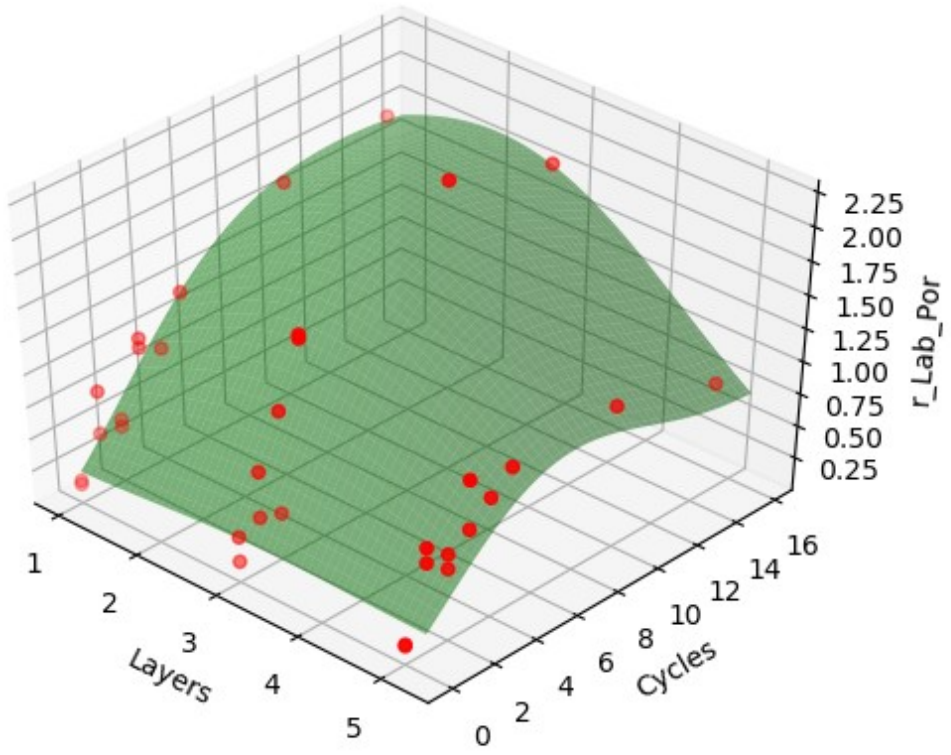

Figure 4. Fitting-ratio between portable and laboratory FTIR 780 cm^{-1} absorbance peak versus number of release agent layers and processing cycles.

If the tool surface history is unknown, fitting-ratios cannot be used to transform portable FTIR results to laboratory measurements. Instead, determining the age of release coating is restricted to analysis of portable results. Fig. 6 shows a GPR surface fit to IR-absorbance peak intensities for the 1020 cm^{-1} peak as a function of the number of RA layers and processing cycles, measured with the portable FTIR. The fitted surface shows a gradual decrease in peak intensity through five cycles, then a plateau through the remainder of the cycles. For a given tool surface, the portable FTIR results can be used to determine if the RA has been aged beyond five cycles or not. This is of course before any noticeable contamination on the tool surface to start affecting the entire FTIR spectrum.

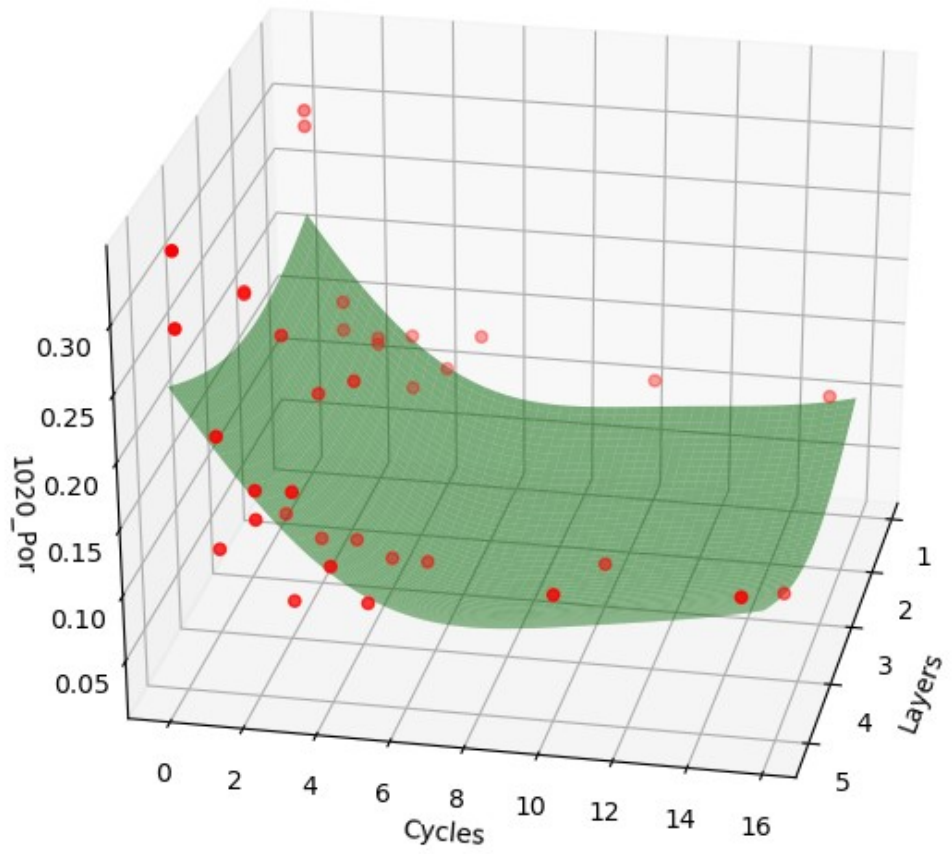

Figure 5. IR-absorbance peak intensity for the 1020 cm^{-1} peak versus number of release agent layers and processing cycles.

3.2 Tool Surface Free Energy

Fig. 6 shows tool SFE versus the number of RA layers and processing cycles for surfaces that underwent no RA reapplications. Red points represent experimental SFE values measured through CAG testing. A response surface, shown in green, was fitted to the data using GPR with an accuracy of 73%. Tool SFEs were measured over an approximate range of 8-15 mJ/m^2. The response surface shows maximum SFE values prior to any autoclave processing cycles for all amounts of RA. The highest pre-processing SFEs were measured on three-layer surfaces, while the lowest values were on one-layer surfaces. Tool SFEs subsequently decreased through the first five cycles, then either plateaued or slightly increased through the fifteen-cycle marks. The slightly higher SFE values measured prior to any autoclave processing suggest that fresh release coatings exhibit lower abhesion properties than slightly-aged coats. This behavior is attributed to the mold surface becoming “conditioned” to the RA [21]. Typically, any substrate with a SFE in the range of 10-60 mJ/m^2 is considered a “low-energy” surface. Although there were slight changes in SFE during processing, values remained well within the low-energy range. The consistently low SFEs indicate the release coating remained highly-abhesive after undergoing fifteen processing cycles without any RA reapplications.

Tool SFE values remained in the approximate range of 8-15 mJ/m^2 regardless of the amount of RA reapplications. Experimental measurements showed a lack of a simple relationship between the independent process variables (i.e., number of RA layers, processing cycles, RA reapplications) and tool SFE. To verify the non-significant interrelationship between process variables and SFE, all experimental data was subjected to an F-test of overall significance using Analysis of Variance (ANOVA). The results from the F-test produced an overall p-value of 0.11, which is greater than the commonly-used significance level of 0.05. Since the p-value was greater than the significance level, it was determined that the interrelationship between the number of RA layers, processing cycles, RA reapplications, and tool SFE was statistically insignificant. Thus, treating a new production tool with greater amounts of RA or intermittently reapplying layers is not necessary to increase the tool's overall abhesive properties within a fifteen-cycle window. Instead, overapplying or reapplying RA layers would only create a reduction in process efficiency.

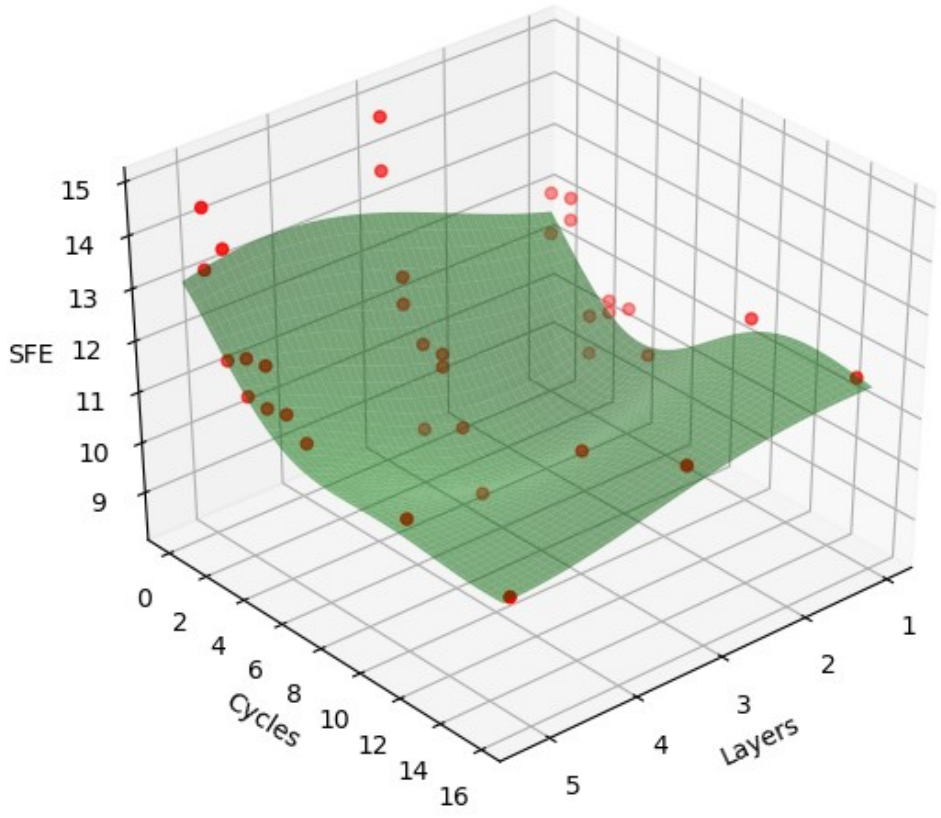

Figure 6. Tool surface free energy (SFE) in mJ/m^2 versus number of release agent (RA) layers and processing cycles. GPR response surface (green) was fit to experimental values (red).

3.3 Tool Surface Contamination

Fig. 7 shows an image of a production tool surface after undergoing fifteen processing cycles without any RA reapplications. The SFE values reported in the figure were measured using the portable CAG technique. The image demonstrates that elevated temperatures and pressures during autoclave processing caused resin to bleed from the prepreg, flow to the tool's outside edges, and cure to the surface. The thickness and surface area of resin contamination increased with each

processing cycle and consequently increased the tool's overall SFE. An increase in SFE promotes tool-part bonding and enhances PIDs in subsequent processing cycles. If tools are not cleaned on a regular basis, contamination levels can continue to grow and be detrimental to end-part quality.

Figure 7. Invar tools used for composites manufacturing after fifteen processing cycles. Surface free energy (SFE) values were measured using the portable CAG set-up.

4. CONCLUSIONS

The first objective of this study was to develop a non-destructive and portable method to evaluate production tool surface condition and the aging of release coating during composites manufacturing in an industrial setting. To achieve this goal, a novel technology based on combined portable experiments and machine learning analysis techniques was developed. A portable tool evaluation set-up was developed using a handheld FTIR and digital microscope to measure surface chemistry and free energy as functions of process variables. Measurements gained through portable methods were used in conjunction with laboratory results to evaluate the aging of release coating. Response surfaces of experimental results were built using Gaussian Process Regression (GPR). The main conclusions from this work are as follows:

Machine learning methods can be used to directly transform portable FTIR measurements into laboratory values if the number of release agent layers and processing cycles are known. If the number of release agent layers and processing cycles are unknown, portable FTIR results can be used to determine an approximate age of release coating, and any contaminations

Release coating remains highly-abhesive after undergoing fifteen processing cycles without any reapplications of release agent. The most significant change in tool surface condition after fifteen processing cycles was the level of resin contamination formed as a border around the part lay-up surface. If parts are not demoldable after fifteen processing cycles, it is likely due to resin contamination build-up, rather than a decrease in release coating abhesion properties.

5. ACKNOWLEDGEMENTS

The work reported here was funded by the Joint Center for Aerospace Technology Innovation (JCATI) and Toray Industries, Inc. The authors would also like to acknowledge Henkel Aerospace

for generously supplying release coating products and the Boeing Company for providing technical expertise and facility access.

6. REFERENCES

1. Zobeiry, N., Forghani, A., Li, C., Gordnian, K., Thorpe, R., Vaziri, R., Fernlund, G., and Poursartip, A. “Multiscale characterization and representation of composite materials during processing.” *Phil. Trans. R. Soc. A,* 374 (2071) (2016): 20150278. doi: 10.1098/rsta.2015.0278.

2. Li, C., Zobeiry, N., Chatterjee, S., and Poursartip, A. “Advances in the characterization of residual stress in composite structures.” *SAMPE Technical Conference Proceedings*. Seattle, WA, June 2-4, 2014. Society for the Advancement of Material and Process Engineering.

3. Twigg, G., Poursartip, A., and Fernlund, G. “Tool–part interaction in composites processing. Part I: experimental investigation and analytical model.” *Composites Part A: Applied Science and Manufacturing* 35(1) (2004): 121-133. doi: 10.1016/S1359-835X(03)00131-3.

4. Twigg, G., Poursartip, A., and Fernlund, G. “Tool–part interaction in composites processing. Part II: numerical modelling.” *Composites Part A: Applied Science and Manufacturing* 35(1) (2004): 135-141. doi: 10.1016/S1359-835X(03)00132-5.

5. Schoenholz, C., Slade, D., Zappino, E., Petrolo, M., Zobeiry, N. “Representation, Characterization, and Simulation of Tool-Part Interaction and Its Effects on Process-Induced Deformations in Composites.” *Proceedings of the 36th American Society for Composites Tech. Conf.* College Station, Texas, September 20-22, 2021. Ed. Ochoa, O. DEStech Publications, Inc. 1204-1216.

6. Potter, K. D., Campbell, M., Langer, C., and Wisnom, M.R. “The generation of geometrical deformations due to tool/part interaction in the manufacture of composite components.” *Composites Part A: Applied Science and Manufacturing*. 36(2) (2005): 301-308. doi: 10.1016/j.compositesa.2004.06.002.

7. Twigg, G., Poursartip, A., and Fernlund, G. “An experimental method for quantifying tool–part shear interaction during composites processing.” *Composites Science and Technology* 63(13) (2003): 1985-2002. doi: 10.1016/S0266-3538(03)00172-6.

8. Ersoy, N., Potter, K., Wisnom, M.R., and Clegg, M.J. “An experimental method to study the frictional processes during composites manufacturing.” *Composites Part A: Applied Science and Manufacturing*. 36(11) (2005): 1536-1544. doi: 1016/j.compositesa.2005.02.010.

9. Zappino, E., Zobeiry, N., Petrolo, M., Vaziri, R., Carrera, E., and Poursartip, A. “Analysis of process-induced deformations and residual stresses in curved composite parts considering transverse shear stress and thickness stretching,” *Composite Structures* 241 (2020): 112057. doi: 10.1016/j.compstruct.2020.112057.

10. Fernlund G., Mobuchon, C., and Zobeiry, N. 2018. “2.3 Autoclave Processing.” *Comprehensive Composite Materials II*. Eds. Beaumont, P.W.R. and Zweben, C.H. Oxford, United Kingdom: Academic Press, 2018: 42-62.

11. Zobeiry, N. and Poursartip, A. “3 - The origins of residual stress and its evaluation in composite materials.” *Structural Integrity and Durability of Advanced Composites*. Eds. Beaumont,

P.W.R., Soutis, C., and Hodzic, A. Sawston, United Kingdom: Woodhead Publishing, 2015. doi: 10.1016/B978- 0-08-100137-0.00003-1.

12. Kaushik, V. and Raghavan, J. “Experimental study of tool–part interaction during autoclave processing of thermoset polymer composite structures.” *Composites Part A: Applied Science and Manufacturing* 41(9) (2010): 1210–1218. doi: 10.1016/j.compositesa.2010.05.003.
13. Albert, C. and Fernlund, G. “Spring-in and warpage of angled composite laminates.” *Composites Science and Technology* 62(14) (2002): 1895–1912. doi: 10.1016/S0266-3538(02)00105-7.
14. Critchlow, G.W., Litchfield, R. E., Sutherland, I., Grandy, D.B., and Wilson, S. “A Review and Comparative Study of Release Coatings for Optimised Abhesion in Resin Transfer Moulding Applications.” *International Journal of Adhesion and Adhesives* 26(8) (2006): 577-599. doi: 10.1016/j.ijadhadh.2005.09.003
15. Blass, D., and Dilger, K. “CFRP-Part Quality as the Result of Release Agent Application – Demoldability, Contamination Level, Bondability.” *Procedia CIRP* 66 (2017): 33–38. doi: 10.1016/j.procir.2017.03.219.
16. Markatos, D.N., Tserpes, K.I., Rau, E., Markus, S., Ehrhart, B., and Pantelakis, Sp. “The effects of manufacturing-induced and in-service related bonding quality reduction on the mode-I fracture toughness of composite bonded joints for aeronautical use.” *Composites Part B: Engineering* 45(1) (2013): 556–564. doi: 10.1016/j.compositesb.2012.05.052.
17. Tracey, A., Flinn, B.D. “Improving adhesive bonding of composites through surface characterization.” *Federal Aviation Administration Joint Advanced Materials and Structures (JAMS) 5th Annual Technical Review Meeting.* CECAM, Wichita State University, July 2009.
18. Tracey, A., Flinn, B.D. “Infrared Spectroscopy: A Potential Quality Assurance Method for Composite Bonding Surface Preparation.” *Proceedings of the International SAMPE Technical Conference Series*. Baltimore, Maryland, May 21-24, 2012.
19. Bainbridge, K., Schoenholz, C., Zobeiry, N. “Investigating the aging of release coating in aerospace composites manufacturing.” *University of Washington Undergraduate Research in Materials Science & Engineering (URMSE)* 2 (2021): 7-11. doi: 10.6069/ssywg443.
20. Henkel Corporation, “TDS Loctite® Frekote® B-15™,” Dec. 2013.
21. Henkel Corporation, “TDS Loctite® Frekote® 710-NC™,” Jan. 2015.
22. de Gennes, P-G., Brochard-Wyart, F., Quere, D. “2. Capillarity and Gravity.” *Capillarity and Wetting Phenomena*. New York, NY: Springer Publishing, 2004. doi: 10.1007/978-0-387-21656-0.
23. Owens, D.K., Wendt, R.C. “Estimation of the surface free energy of polymers.” *Journal of Applied Polymer Science* 13 (1969): 1741-1747.